

## LETTERS

### Organic Solvent Dispersions of Single-Walled Carbon Nanotubes: Toward Solutions of Pristine Nanotubes

Kevin D. Ausman,<sup>†</sup> Richard Piner, Oleg Lourie, and Rodney S. Ruoff\*

Department of Physics, Washington University, CB 1105, One Brookings Drive,  
St. Louis, Missouri 63130-4899

Mikhail Korobov

Department of Chemistry, Moscow State University, Moscow 119899, Russia

Received: July 19, 2000

A systematic study has been performed in order to find an appropriate medium for solubilization/dispersion of pristine single-walled carbon nanotubes (SWCNTs). Five solvents, all featuring high electron pair donicity ( $\beta$ ) and low hydrogen bond parameter ( $\alpha$ ) have demonstrated the ability to readily form stable dispersions. The best dispersions have been characterized by UV/visible-NIR spectra, ESR spectra, and atomic force microscopy (AFM).

Single-walled carbon nanotubes (SWCNTs) have been proposed as promising materials for a variety of applications, including molecular electronics<sup>1</sup> and polymer reinforcement.<sup>2</sup> For many of these applications, however, solution-phase handling would be exceptionally useful. SWCNTs have been solubilized in water with the aid of surfactants,<sup>3</sup> and have even been purified and length-selected in this form,<sup>4,5</sup> but removing the surfactant afterward is problematic. SWCNTs have been solubilized by functionalizing the end-caps with long aliphatic amines.<sup>6</sup> This approach apparently works well, but has the disadvantage that the most convenient chemical "handles" for further modification, the acid-treated end-caps, are tied-up by the solubilization functionality. Further, it has been reported that SWCNTs have been solubilized by functionalizing their sidewalls with fluorine<sup>7</sup> and with alkanes.<sup>8</sup> In both of these latter

cases, the sidewall functionalization coverage is high, resulting naturally in a modification of the intrinsic SWCNT properties.<sup>9,10</sup>

To avoid these problems, it would be desirable to find solvents capable of solvating the pristine tubes. To date, the best solvents reported for generating SWCNT dispersions are amides, particularly *N,N*-dimethylformamide (DMF) and *N*-methylpyrrolidone (NMP).<sup>8,11</sup> Although the work cited reports the DMF dispersions to be "stable suspensions", our recent results suggest that these dispersions aggregate on a time-scale of days. The work reported here is an attempt to elucidate the solvation of SWCNTs in the hopes of pointing the way toward better solvents.

Purified single-walled carbon nanotube (SWCNT) material was obtained from Tubes@Rice (Rice University, Houston, TX) in two forms, Triton X-100 solution and toluene dispersion. In both cases, free-standing bucky-paper was made from the starting materials by slight modifications to standard procedures.<sup>3</sup> The SWCNT material was suction-filtered through Whatman Anodisc 47 filters (20 nm pore size), was washed with water and methanol, and was then dried in air at 130 °C

\* Author to whom correspondence should be addressed: E-mail: ruoff@wuphys.wustl.edu. As of September, 2000, Dept. of Mechanical Engineering, Northwestern University, 2145 Sheridan Road, Evanston, Ill 60208-3111.

<sup>†</sup> Present address: Department of Chemistry, MS-60, Rice University, P.O. Box 1892, Houston, TX 77005-1892.

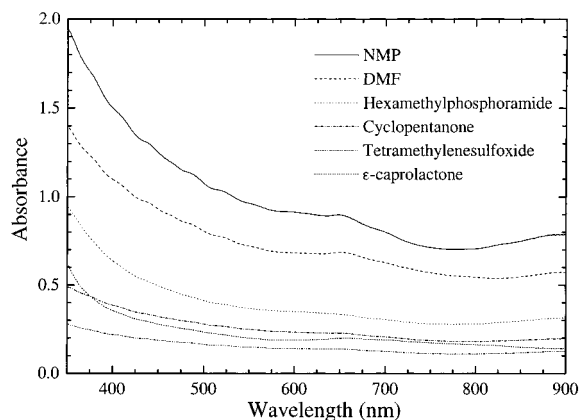


**Figure 1.** UV/visible spectra of SWCNT material dispersions in the “best” solvents.

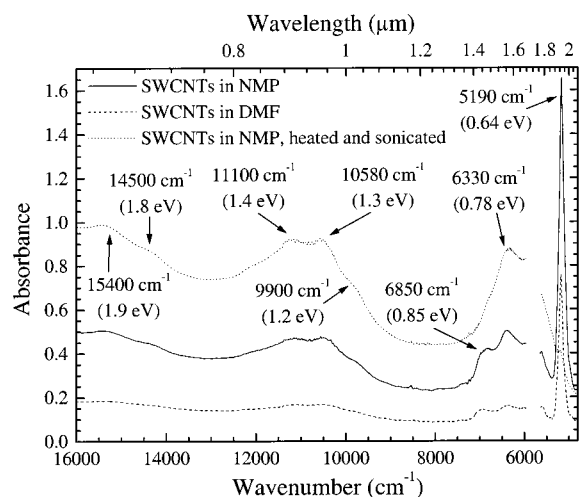


**Figure 2.** Visible and near-infrared spectrum of SWCNT material dispersed in NMP and DMF. The gap in the spectra near  $6000\text{ cm}^{-1}$  is due to solvent absorbance in this region.

for 15 min to drive off residual surfactant. The bucky-paper made from the Triton X-100 solution was highly smooth and mechanically robust, and when redispersed in DMF and imaged by contact-mode atomic force microscopy (AFM) after drying droplets onto substrates the SWCNTs were observed to be very clean except for the ever-present residual catalyst particles. The bucky-paper made from the toluene dispersion, on the other hand, had a felt-like appearance, and the SWCNTs were markedly “dirtier” when investigated by AFM in the same manner. We propose that the quality of the dispersion in Triton X-100 is very high, producing a uniformly intertwined bucky-paper, whereas the dispersion in toluene consists primarily of large aggregates of SWCNTs, producing a paper that is a more loosely connected assembly of tightly bound aggregates. This accounts for the observed lower mechanical strength and different appearance. The solvents in the washing steps on this latter type of paper can be expected to pass primarily between these initial aggregates, resulting in the observed poorer cleanliness. All further experiments reported here used bucky-paper produced from Triton X-100 solutions.

Obvious excesses of SWCNT bucky-paper were dispersed by bath sonication in the thirteen solvents studied, which had a range of solvent parameters.<sup>12</sup> The solvents were commercial samples from Aldrich and Alpha-Aesar, and were used without additional purification. In a second series of experiments, the dispersions in the two most promising solvents, NMP and DMF, were additionally sonicated for 5 h at  $60\text{ }^{\circ}\text{C}$ .

To distinguish the poor dispersion of large aggregates from the suspension or solution of individual SWCNTs and ropes, the resulting dispersions were centrifuged for 30 min at room temperature. The UV/visible and near-infrared (NIR) spectra of the liquid phases separated by centrifugation were taken. Some samples were further examined by electron spin resonance (ESR) spectroscopy, and by noncontact atomic force microscopy (NC-AFM) of dried droplets on glass microscope slides.

The solvents investigated can be divided into three groups on the basis of the UV/visible spectra of their SWCNT dispersions. The “best” solvents, NMP, DMF, hexamethylphosphoramide, cyclopentanone, tetramethylene sulfoxide, and  $\epsilon$ -caprolactone (listed in decreasing order of optical density of the resulting dispersions), readily disperse SWCNTs, forming light-gray, slightly scattering liquid phases. All of these solvents are characterized by high values for  $\beta$  (electron pair donicity), negligible values for  $\alpha$  (the hydrogen bond donation parameter of Taft and Kamlet), and high values for  $\pi$  (solvochromic parameter).<sup>12</sup> Thus, Lewis basicity (i.e., the availability of a free electron pair) without hydrogen donors is key to good solvation of SWCNTs.

The UV/visible spectra of the dispersions in this category exhibited unresolved structure between 350 and 600 nm and a resolved, broad peak at 650 nm (see Figure 1). The near-infrared spectra of the dispersions in NMP and DMF were also taken (see Figure 2), exhibiting features that are compared to electronic transitions in SWCNTs taken from the literature (Table 1). The observed spectral features fall into three main categories: the visible absorption peaks near 650–690 nm (1.9–1.8 eV), the near-infrared absorption peaks near 900–1000 nm (1.4–1.2 eV), and the near-infrared absorption peaks near 1450–1930 nm (0.85–0.64 eV). The first of these categories, the visible peaks, consists of a primary feature at 650 nm (1.9 eV), a shoulder at 690 nm (1.8 eV), and possibly the unresolved structure to the blue of these peaks. This region matches well to the interband transitions attributed to metallic nanotubes.<sup>1,13–15</sup> These features contrast with the smooth, featureless visible absorption spectrum reported for chemically solubilized SWCNTs,<sup>6,16</sup> perhaps suggesting differing reactivity between the metallic and semiconducting SWCNTs in those studies. Jost et al., observing a similarly resolved spectrum, attribute the multiple discrete absorption peaks to tubes of different diameters, present in discrete jumps of  $0.07\text{ nm}$ .<sup>15</sup>

The third category mentioned above consists of a sharp peak near 1930 nm, and two slightly broader peaks near 1565 and 1460 nm. It is likely that our unfortunate spectral gap near 1800 nm produced by a solvent absorption in that region hides the presence of yet another resolved peak. These transitions are thought to reflect the band gap of semiconducting SWCNTs.<sup>1,6,13</sup> Unlike the other spectral regions they investigated, Jost et al. observed a broad peak centered around  $0.75\text{ eV}$  in this region.<sup>15</sup> The most pronounced spectral feature in this range, at  $0.64\text{ eV}$ , is remarkable in its sharpness, with a Lorentzian width of only  $0.01\text{ eV}$ . This also contrasts markedly with the feature observed in this spectral region on chemically solubilized SWCNTs, which was significantly wider (approximately  $0.12\text{ eV}$ ).<sup>6,16</sup> Perhaps this indicates a much narrower range of band gaps contributing to this transition than might be otherwise expected.

Upon attempting to drive more SWCNT material into the NMP dispersion, the relative intensities of the peaks in this region shifted; the 1450 nm peak became a shoulder on the larger 1580 nm peak, and 1930 nm peak nearly disappeared. The origin of this effect is currently unknown, but is almost certainly a result of more than simply differing solubilities of

TABLE 1: Electronic Transitions in SWCNTs<sup>a</sup>

peaks, nm, (eV)	method	type of sample	refs
2480–2066, (0.5–0.6) 729–619, (1.7–2.0)	STM, STS	individual tubes	13
1907, (0.65 ± 0.05) 1033, (1.2 ± 0.1) 689, (1.8 ± 0.1)	EELS	solid, Cu grids	1
1653, (0.75) 689, (1.8) 652, (1.9) 925, (1.34)	NIR	soot–methanol mixture, sprayed onto a quartz plate	15
1844, (0.67) 1103, (1.12) 1031, (1.20) 948, (1.31)	NIR	SWCNT –CONH-4-C <sub>6</sub> H <sub>4</sub> (CH <sub>2</sub> ) <sub>13</sub> CH <sub>3</sub> solution in CS <sub>2</sub> , 3.3 mg/mL	16
1855, (0.67) 1097, (1.13) 1031, (1.20) 973, (1.27)	NIR	SWCNT –COO <sup>-</sup> +NH <sub>3</sub> (CH <sub>2</sub> ) <sub>17</sub> CH <sub>3</sub> solution in THF	16
1855, (0.67) 1090, (1.14) 1021, (1.21)	NIR	SWCNT –CONH(CH <sub>2</sub> ) <sub>17</sub> CH <sub>3</sub> solution in CS <sub>2</sub>	6
1948, (0.64), max 1896, (0.65) 1827, (0.68) 1098, (1.13) 1022, (1.21) 938, (1.32)	NIR	SWCNT –CONH-4-C <sub>6</sub> H <sub>4</sub> (CH <sub>2</sub> ) <sub>13</sub> CH <sub>3</sub> solution in pyridine, 1.7 mg/mL, part, soluble in pyridine only	16
1930, (0.64) 1575, (0.79) 1450, (0.86) 950, (1.31) 900, (1.38) 650, (1.91)	NIR	solution/dispersion in DMF, pristine SWCNTs	this study
1934, (0.64) 1565, (0.79) 1460, (0.85) 950, (1.31) 900, (1.38) 650, (1.91)	NIR	solution/dispersion in NMP, pristine SWCNTs	this study
1928, (0.64) 1580, (0.78) 945, (1.31) 900, (1.38) 648, (1.91)	NIR	solution/dispersion in NMP, pristine SWCNTs, extensive heating/sonication	this study

<sup>a</sup> From the literature.

the different SWCNT diameters, since such an explanation would require a markedly decreased solubility of the species producing the 1930 nm feature with increasing temperature and sonication. A similar attempt to drive more SWCNT material into the DMF dispersion was unsuccessful, resulting in significantly poorer resolution in the NIR spectrum. AFM images showed the appearance of “ball-like” particles in this case.

The second, intermediate category of peaks mentioned above, ranging from 900 to 1000 nm, are attributed in the literature variously to either metallic or semiconducting SWCNTs.<sup>1,6,15,16</sup> As in the first case above, Jost et al. attribute these resolved absorption peaks to discrete diameters of SWCNTs.<sup>15</sup> In both cases, our observed spectral line positions match those reported in Jost et al. However, the tracking of these spectral intensities with the unambiguously metallic transitions near 650 nm as more material is forced into the dispersion by continued heating and sonication contrasts with the shifts in intensities observed for the unambiguously semiconducting tube transition near 0.64 eV, thus suggesting that these intermediate transitions arise from

secondary metallic SWCNT transitions. This observation is in agreement with Chen et al.,<sup>6</sup> but not with Jost et al.<sup>15</sup>

From this analysis, we can deduce that the Tubes@Rice material studied here consists primarily of discrete diameters of both metallic and semiconducting SWCNTs, whereas the material studied by Jost et al. contained a more continuous distribution of semiconducting SWCNT diameters.<sup>15</sup> The absence of the 1.9 eV transitions in the chemically solubilized SWCNTs of Chen et al. and Hamon et al. is puzzling; however, the shifts to lower energy of the other two transition areas is consistent with larger average diameter SWCNTs in these samples than were investigated here.<sup>6,16</sup>

Both DMF and NMP dispersions were EPR silent. This is in agreement with Chen et al., who observed no EPR signal for water and ethanol dispersions of pristine SWCNTs and found a weak signal for chemically purified SWCNTs in the same solvents. Shortened tubes, however, gave a strong ESR signal with  $g = 2.00$ .<sup>17</sup>

A second class of UV/visible spectra, featureless but for a

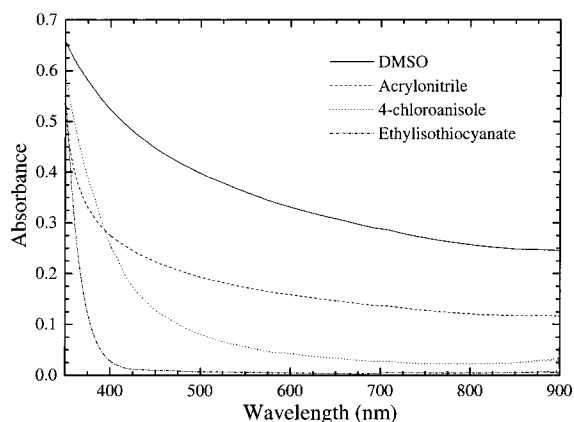


**Figure 3.** Featureless UV/visible spectra of SWCNT material dispersions.

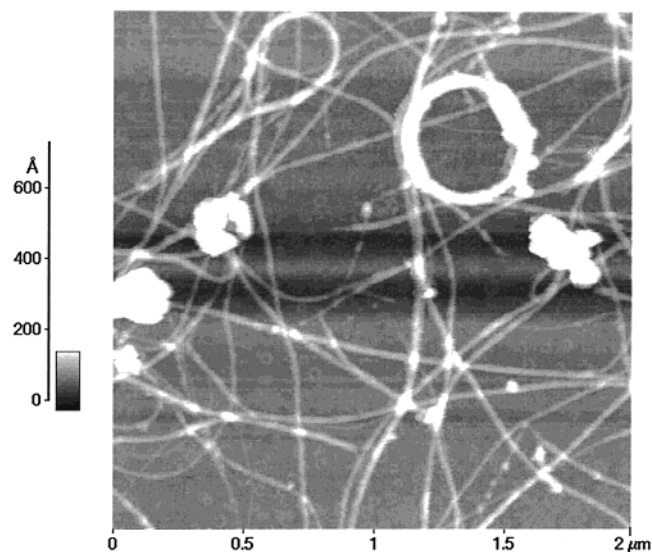


**Figure 4.** Noncontact AFM image of SWCNT material dispersed on a glass substrate from DMF dispersion.

gradually increasing extinction toward the ultraviolet, were observed for dispersions in dimethyl sulfoxide (DMSO), acrylonitrile, 4-chloroanisole, and ethylisothiocyanate (Figure 3). A third class of spectra exhibiting only fullerene-like features was observed for dispersions in 1,2-dichlorobenzene, 1,2-dimethylbenzene, bromobenzene, iodobenzene, and toluene, solvents known to be exceptional for  $C_{60}$  and  $C_{70}$ .<sup>18</sup>

To evaluate representative samples of each solvent category as determined by UV/visible spectroscopy, single drops of the centrifuged dispersions of SWCNT material in DMF, 4-chloroanisole, and toluene were dried overnight on glass microscope slides. These substrates were then imaged by noncontact AFM.

The DMF dispersion showed a high density of SWCNTs and ropes intertwined on the glass surface, confirming that the majority of the material dispersed was in fact nanotube material (Figure 4). This sample also contained a higher relative density of impurities than the starting material, supporting the intuitive notion that the impurities, largely catalytic particles, would have a greater solubility relative to SWCNTs in most solvents than the relative composition of the starting material, and thus would be concentrated by the described procedure. The 4-chloroanisole dispersion showed a high density of impurities and very few SWCNTs or ropes. The toluene sample had large crystallized regions with observable step-edges, consistent with a moderate concentration of fullerenes extracted as impurities from the SWCNT sample.

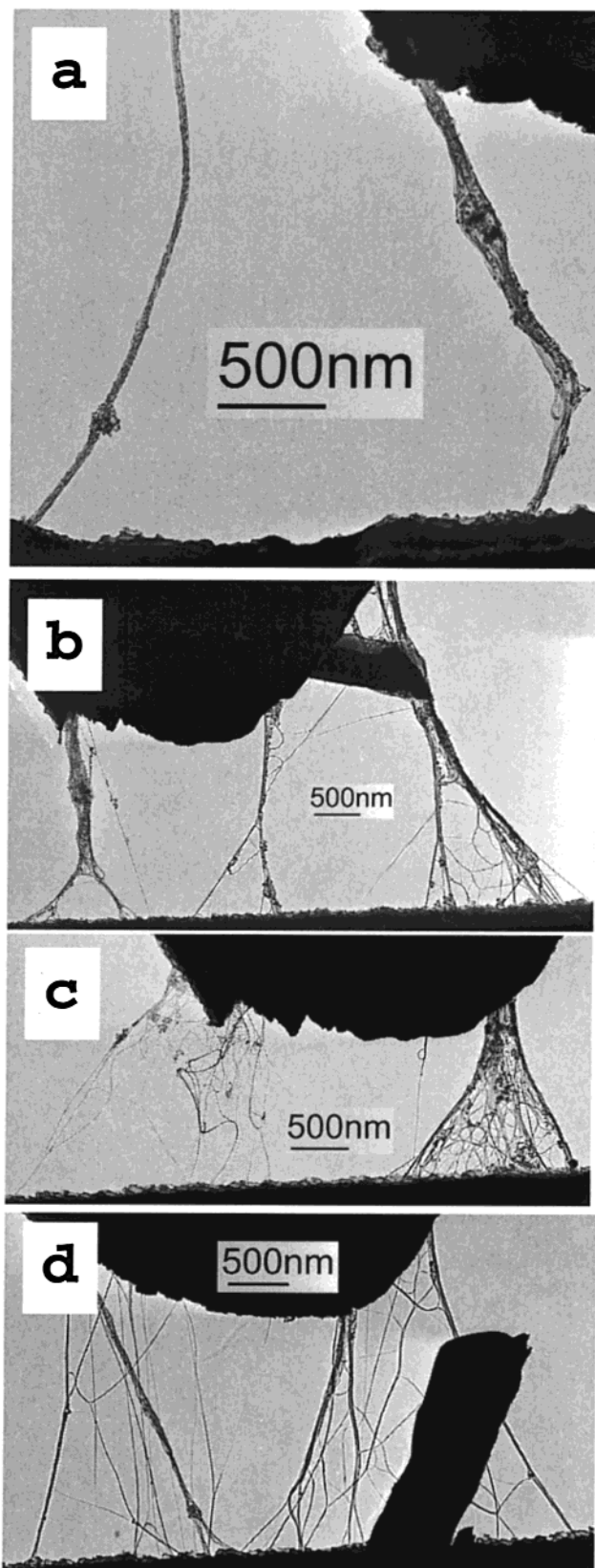


**Figure 5.** TEM images of SWCNTs dispersed across a gap etched through silicon. (a) Dispersed in DMF. (b) Dispersed to saturation in NMP and diluted 1:9 by DMF. (c) Dispersed to saturation in NMP and diluted 1:(1:8) by (NMP:DMF). (d) Dispersed to saturation in NMP and diluted 1:9 by NMP.

Microdroplets of NMP, DMF, and mixed NMP:DMF dispersions of SWCNT material were deposited by micropipet across an etched gap in a silicon wafer, allowed to dry, and then imaged

by transmission electron microscopy (TEM). In all cases, small ropes and individual tubes spanned the gap; however, the more NMP present, the more the dispersion resulted in spanning tubes that were clean of adhering catalytic particles (Figure 5), suggesting greater solubilization in the case of NMP.

In comparing the observed trends in solubilization reported in this paper to various solubility parameters, some trends become apparent. The best solvents studied, NMP and DMF, have high values for  $\beta$  (the hydrogen bond acceptance basicity), negligible values for  $\alpha$  (the hydrogen bond donation parameter of Taft and Kamlet), and high values for  $\pi^*$  (solvochromic parameter).<sup>12</sup> This indicates that Lewis basicity without hydrogen donors is key to good solvation of SWCNTs. However, this seems to be a necessary but not sufficient set of conditions, as DMSO, a mediocre solvent, meets those criteria.

In summary, we have investigated the room-temperature solubility of SWCNTs in a variety of solvents, finding a class of non-hydrogen-bonding Lewis bases that provide good solubility. The absorption spectra match what is expected from the known band structure of the SWCNTs. The observed remarkable narrowness of the 0.64 eV peak, attributed to the band-gap of semiconducting SWCNTs, is currently unexplained.

**Acknowledgment.** The authors (K.D.A., R.P., O.L., R.S.R.) gratefully acknowledge the financial support of ONR/DARPA. R.S.R. and M.V.K. additionally acknowledge financial support from NATO. M.V.K. was further supported in this work by the RFBR grant 000332097 and by the Russian State Program, "Fullerenes and Atomic Clusters". The experimental assistance of Christine Kirmaier, Dewey Holton, and T. C. Yang is gratefully acknowledged.

## References and Notes

(1) Pichler, T.; Knupfer, M.; Golden, M. S.; Fink, J.; Rinzler, A.; Smalley, R. E. *Phys. Rev. Lett.* **1998**, *80*, 4729–4732.

(2) Andrews, R.; Jacques, D.; Rao, A. M.; Rantell, T.; Derbyshire, F.; Chen, Y.; Chen, J.; Haddon, R. C. *Appl. Phys. Lett.* **1999**, *75*, 1329–1331.

(3) Liu, J.; Rinzler, A. G.; Dai, H. J.; Hafner, J. H.; Bradley, R. K.; Boul, P. J.; Lu, A.; Iverson, T.; Shelimov, K.; Huffman, C. B.; Rodriguez-Macias, F.; Shon, Y. S.; Lee, T. R.; Colbert, D. T.; Smalley, R. E. *Science* **1998**, *280*, 1253–1256.

(4) Krstic, V.; Duesberg, G. S.; Muster, J.; Burghard, M.; Roth, S. *Chem. Mater.* **1998**, *10*, 2338–2340.

(5) Duesberg, G. S.; Muster, J.; Krstic, V.; Burghard, M.; Roth, S. *Appl. Phys. A: Mater. Sci. Process.* **1998**, *A67*, 117–119.

(6) Chen, J.; Hamon, M. A.; Hu, H.; Chen, Y.; Rao, A. M.; Eklund, P. C.; Haddon, R. C. *Science* **1998**, *282*, 95–98.

(7) Mickelson, E. T.; Chiang, I. W.; Zimmerman, J. L.; Boul, P. J.; Lozano, J.; Liu, J.; Smalley, R. E.; Hauge, R. H.; Margrave, J. L. *J. Phys. Chem. B* **1999**, *103*, 4318–4322.

(8) Boul, P. J.; Liu, J.; Mickelson, E. T.; Huffman, C. B.; Ericson, L. M.; Chiang, I. W.; Smith, K. A.; Colbert, D. T.; Hauge, R. H.; Margrave, J. L.; Smalley, R. E. *Chem. Phys. Lett.* **1999**, *310*, 367–372.

(9) Brenner, D. W. S., J. D.; Mewkill, J. P.; Shenderova, O. A. *J. Br. Int. Soc.* **1998**, *51*, 137.

(10) Garg, A.; Sinnott, S. B. *Chem. Phys. Lett.* **1998**, *295*, 273–278.

(11) Liu, J.; Casavant, M. J.; Cox, M.; Walters, D. A.; Boul, P.; Lu, W.; Rimberg, A. J.; Smith, K. A.; Colbert, D. T.; Smalley, R. E. *Chem. Phys. Lett.* **1999**, *303*, 125–129.

(12) Marcus, Y. *J. Solution Chem.* **1991**, *20*, 929–944.

(13) Wildoer, J. W. G.; Venema, L. C.; Rinzler, A. G.; Smalley, R. E.; Dekker, C. *Nature (London)* **1998**, *391*, 59–62.

(14) Odom, T. W.; Huang, J.-L.; Kim, P.; Ouyang, M.; Lieber, C. M. *J. Mater. Res.* **1998**, *13*, 2380–2388.

(15) Jost, O.; Gorbunov, A. A.; Pompe, W.; Pichler, T.; Friedlein, R.; Knupfer, M.; Reibold, M.; Bauer, H.-D.; Dunsch, L.; Golden, M. S.; Fink, J. *Appl. Phys. Lett.* **1999**, *75*, 2217–2219.

(16) Hamon, M. A.; Chen, J.; Hu, H.; Chen, Y.; Itkis, M. E.; Rao, A. M.; Eklund, P. C.; Haddon, R. C. *Adv. Mater.* **1999**, *11*, 834–840.

(17) Chen, Y.; Chen, J.; Hu, H.; Hamon, M.; Itkis, M.; Haddon, R. *Chem. Phys. Lett.* **1999**, *299*, 532–535.

(18) Korobov, M. V.; Mirakyan, A. L.; Avramenko, N. V.; Olofsson, G.; Smith, A. L.; Ruoff, R. S. *J. Phys. Chem. B* **1999**, *103*, 1339–1346.